Partial Recovery of Dynamic R_{ON} vs OFF-State Stress Voltage in p-GaN Gate AlGaN/GaN Power HEMTs

Marcello Cioni, *Student Member, IEEE*, Nicolò Zagni, *Graduate Student Member, IEEE*, Ferdinando Iucolano, Maurizio Moschetti, Giovanni Verzellesi, *Senior Member, IEEE*, and Alessandro Chini

***Abstract*—Dynamic R_{ON} dispersion due to buffer traps is a well-known issue of GaN power HEMTs, critically impacting their performance and stability. Several works show that the dynamic R_{ON} reaches a maximum for some off-state drain-source voltage ($V_{DS,OFF}$) value typically in the range of several hundred volts and then partially recovers to smaller values. In this work, we propose a quantitative explanation for this behavior, attributing it to the charging/discharging dynamics of Carbon-related buffer traps. We characterize the dynamic R_{ON} in packaged p-GaN gate AlGaN/GaN HEMTs with a custom measurement setup. We find that in these devices the relative R_{ON} increase reaches a maximum of 60% for $V_{DS,OFF} \approx$ 100-200 V, partially recovering to about 30% as $V_{DS,OFF}$ is raised to 500 V. We ascribe this behavior to the partial neutralization of C-related acceptor traps in the buffer due to trapping of holes produced by a high-field generation mechanism. This explanation is supported by calibrated 2D numerical simulations, that successfully reproduce the experimentally observed R_{ON} reduction only when including a hole generation mechanism.**

***Index Terms*—p-GaN HEMTs, Dynamic ON-Resistance, Carbon Doping, "Hole-Redistribution" Model**

I. Introduction

NORMALLY-off operation (i.e., positive threshold voltage, V_T) in AlGaN/GaN high electron mobility transistors (HEMTs) is highly desirable to simplify circuit design and for safety considerations [1]. Among technology solution that make this possible [2], p-GaN gate devices represent a very promising solution [3], [4]. Despite the huge academic and industrial interest in GaN HEMTs for power applications due to their high current and voltage capability [2], [5], critical issues related to device stability and reliability still need to be fully understood [1]. Among these, particular interest has been devoted to analyze V_T instability and dynamic ON-Resistance (R_{ON}) degradation [6], [7], both being critical parameters influencing performance.

M. Cioni, N. Zagni, and A. Chini are with the Department of Engineering "Enzo Ferrari", Università di Modena e Reggio Emilia, 41125, Modena, Italy. (M. Cioni and N. Zagni contributed equally to this work.) (e-mail: nicolo.zagni@unimore.it).
F. Iucolano and M. Moschetti are with STMicroelectronics, Catania, 95121, Italy.
G. Verzellesi is with Department of Sciences and Methods for Engineering (DISMI) and EN&TECH Center, University of Modena and Reggio Emilia, 42122, Reggio Emilia, Italy.

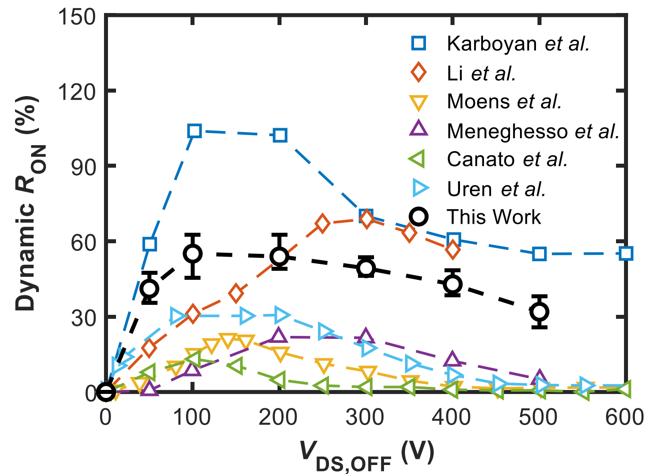

Fig. 1. Dynamic R_{ON} vs $V_{DS,OFF}$ data found in the literature [7], [17], [19]–[21] and obtained from our measurements (see legend). The partial recovery behavior is observed on different GaN power HEMT technologies.

One of the main sources of dynamic dispersion is the charging and discharging of buffer traps as a result of OFF-to-ON switching, and vice-versa [1], [8]–[11]. Buffer traps are typically related to the impurities intentionally introduced during device fabrication – such as Iron (Fe) or Carbon (C) – to reduce the off-state leakage and increase the breakdown voltage [8], [12], [13]. At the same time, however, the introduction of these traps make the device more prone to current-collapse effects and dynamic R_{ON} degradation [9]–[11], [14]–[16]. A widely reported – yet not definitely assessed – result in the literature is the non-monotonic dependence of R_{ON} on the adopted off-state drain voltage ($V_{DS,OFF}$), that has indeed been

© 2021 IEEE. Personal use of this material is permitted. Permission from IEEE must be obtained for all other uses, in any current or future media, including reprinting/republishing this material for advertising or promotional purposes, creating new collective works, for resale or redistribution to servers or lists, or reuse of any copyrighted component of this work in other works.

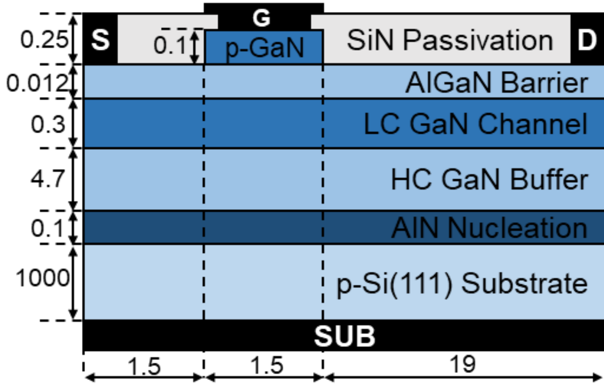

Fig. 2. Sketch of the measured and simulated p-Gate GaN HEMT structure (not to scale). All dimensions are indicated in μm.

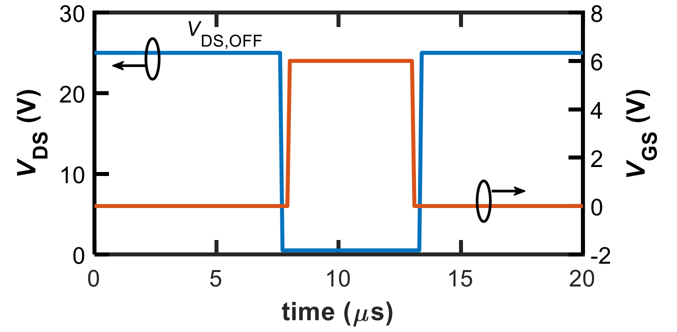

Fig. 3. Typical V_{DS} and V_{GS} signals applied during the switch-mode characterization for monitoring dynamic R_{ON} evolution.

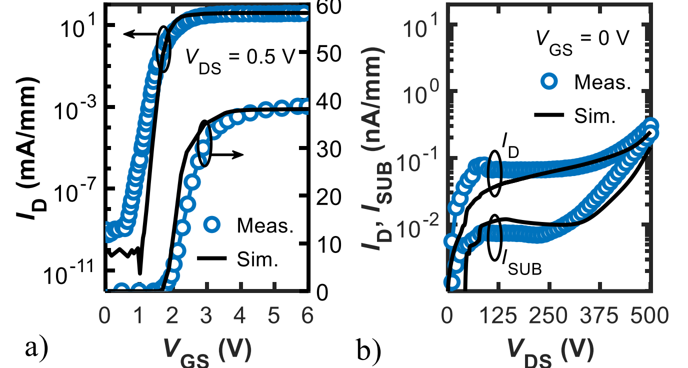

Fig. 4. Comparison between measured (blue dots) and simulated (black solid lines) (a) I_D-V_{GS} curves and (b) I_D, I_{SUB}-V_{DS} in the off-state.

observed in different AlGaN/GaN power HEMT technologies [7], [17]–[21]. Some of this literature data is collected and shown in Fig. 1.

While dynamic R_{ON} degradation is generally attributed to dispersion effects due to buffer traps, different interpretations for the observed partial recovery have been proposed:

1. balancing of negative and positive buffer charge storage [19], [22] induced by leakage paths between the 2DEG and the carbon-doped buffer (either accounted for through heavily p-doped shorts [10], [17], [21] or band-to-band hopping transport [23]),
2. generation of positive charge by ionization of donor traps in the UID GaN channel layer [24],
3. charge redistribution within the structure due to increasing vertical drain-to-substrate leakage [25],
4. partial reduction of negative substrate potential due to leakage of electrons from the substrate to the buffer and drain contact (applicable only to floating substrate conditions) [26],
5. positive charge storage at the interface between the carbon-doped buffer and the strain-relief layers/nucleation layer due to the neutralization of ionized acceptors or to ionization of donors [10], [21]–[23], [25].

Nonetheless, a consistent and quantitative interpretation for the observed partial recovery of dynamic R_{ON} is still lacking.

In this work, we present experimental data confirming the partial recovery of dynamic R_{ON} vs $V_{DS,OFF}$ in packaged p-GaN gate AlGaN/GaN HEMTs, and we analyze this phenomenon by means of calibrated 2D numerical device simulations. Simulations suggest that the observed behavior can be attributed to the partial neutralization of buffer acceptor traps (related to Carbon doping) induced by impact-ionization generated holes. Part of these holes get captured by acceptor states in the buffer, thus reducing the negatively ionized acceptors in the access region near the drain, this in turn allowing for the partial recovery of R_{ON} as observed in the experiments.

The paper is organized as follows. In Section II, a description of the devices under test is provided. In Section III, we illustrate the adopted stress measurement methodology and the simulation setup. Results are presented and discussed in Section IV. Finally, conclusions are drawn in Section V.

II. Devices Description

Tested devices are packaged p-GaN gate AlGaN/GaN HEMTs grown by metal–organic chemical vapor deposition on a p-type Si substrate. A schematic view of the device cross-section is shown in Fig. 2. The channel is composed of a Low-Carbon-doped (LC, ~10^{16} cm^{-3}) GaN layer of 0.3 μm. The GaN buffer layer instead is 4.7 μm thick and is highly C-doped (~10^{18} cm^{-3}). The AlGaN barrier layer is 15 nm thick with 22% Al concentration. The *p*-type GaN layer is 100 nm thick and has a nominal Mg doping concentration in the range of 10^{19}–$5{\times}10^{19}$ cm^{-3}. To define the p-Gate region, a Cl-based plasma etch was carried out [27]. The gate length is 1.5 μm. The depletion region forming due to the p-i-n diode corresponding to the pGaN/AlGaN/GaN heterostructure effectively suppresses the 2DEG when no gate bias is applied thus obtaining $V_T > 0$ V. Ohmic contacts were formed by Ti/Al-based metallization defined by means of a lift-off process [28]. Nominal 2DEG density and mobility are $8.6{\times}10^{12}$ cm^{-2} and 1400 cm^2/(V·s), respectively [29]. The characterization was performed on different devices finding good measurement repeatability.

III. Methods

A. Measurement Methodology

The switch-mode stability of devices under study was characterized by means of a custom measurement setup, described in [30]. OFF-state stresses were applied with increasing $V_{DS,OFF}$ values in the 50–500 range and V_{GS} = 0 V up to a total stress time (t_{OFF}) of 1000 s for each $V_{DS,OFF}$ value. The substrate contact is electrically shorted to the source contact inside the package. Before starting this stability

TAB. I CHYNOWETH'S LAW COEFFICIENTS FOR IMPACT IONIZATION IN GAN AS OBTAINED FROM MONTE CARLO SIMULATIONS [37]

Parameter	Value
a_n (electrons)	3.46×10^{6} cm^{-1}
b_n (electrons)	1.58×10^{7} V/cm
a_p (holes)	6.15×10^{6} cm^{-1}
b_p (holes)	1.69×10^{7} V/cm

characterization, the static R_{ON} was measured ($V_{GS,}$ V_{DS}) = (6, 0.5) V to set the reference value (R_{ON0}). During OFF-state stress, the Device Under Test (DUT) was periodically turned-on to monitor the dynamic R_{ON} evolution over a 10^{-3}–10^{3} s time range. To this end, a short (5 µs) low drain bias (0.5 V) was applied to the DUT at logarithmically spaced time intervals, during which V_{GS} was pulsed to 6 V to bring the DUT in its triode region (see Fig. 3). High/low and low/high drain voltage transitions were performed at negligible current (i.e., under soft-switching conditions) to avoid hot electrons effect that might increase the R_{ON} degradation at high $V_{DS,OFF}$ [31]. R_{ON} was thus computed as the ratio between the measured V_{DS} and I_D averaged over each 5 µs low voltage drain pulse.

B. Simulation Setup

The simulated device is sketched in Fig. 2, which resembles the DUT structure. The two-dimensional (2D) numerical device simulations were carried out with SDevice™ simulator (Synopsys Inc.) [32]. The simulation deck was calibrated against measured DC I_D–V_{GS} and I_D, I_{SUB}–V_{DS} in the off-state (V_{GS} = 0 V) as shown in Fig. 4(a) and (b), respectively (measurement data in Fig. 4 were obtained from on-wafer devices with the same specifications as those of the packaged devices described in Section II).

Charge transport was simulated by means of the drift-diffusion model. The default strain model of the simulator was used to include the piezoelectric polarization at the heterointerfaces [32]. Similarly to previous TCAD studies [6], [33], incomplete ionization of magnesium acceptors was taken into account in the p-GaN gate region (the Mg ionization energy was set to 0.16 eV from the GaN valence band edge). A fully dynamic trap modeling approach was adopted, with one Shockley-Read-Hall (SRH) trap-balance equation for each level, describing the trap-occupation dynamics without any quasi-static approximation. A detailed description of the device physics modeling approach in AlGaN/GaN HEMTs can be found in [34]. To model the vertical leakage conduction through the substrate and nucleation layers, we employed a similar strategy to that discussed in [35], [36]. Impact-ionization coefficients for both electrons and holes in the GaN layers were set in agreement with recent Monte-Carlo calculations [37], and are reported in Tab. I.

C doping in the GaN buffer was modeled by considering a dominant deep acceptor trap at 0.9 eV above E_V [38], [39] partially compensated by a shallow donor trap at 0.11 eV below E_C [40]. To reproduce the experimental results, the adopted trap concentrations were 4.3×10^{17} cm^{-3} and 4×10^{17} cm^{-3}, for C-related acceptors and donors, respectively. This corresponds to an effective acceptor density of 3×10^{16} cm^{-3} (about 1% of the nominal C-doping concentration in the buffer [41]). No additional traps were considered, while in all nitride layers an n-type doping density of 10^{15} cm^{-3} was assumed to account for the unintentional n-type conductivity due to shallow-donor impurities incorporated during growth [12], [42].

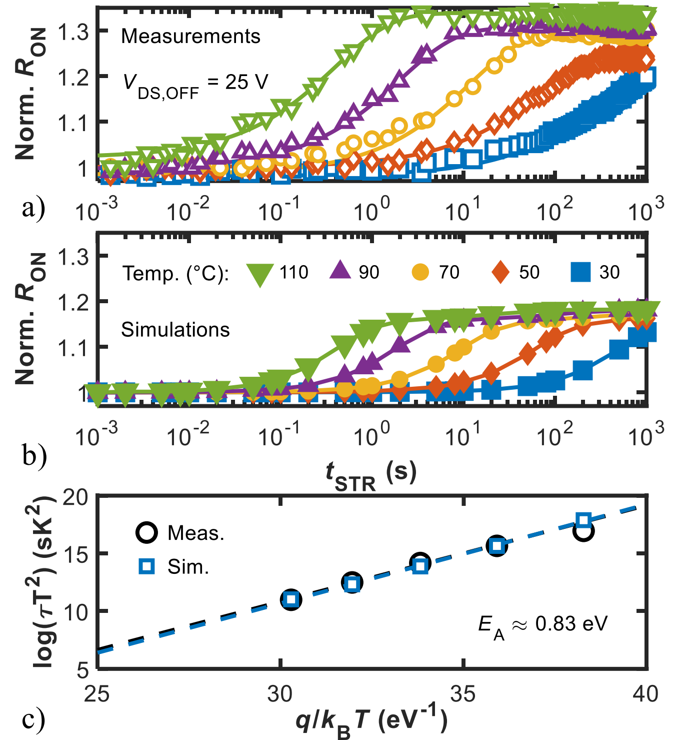

Fig. 5. a) Measured and b) simulated normalized R_{ON} transients at different temperatures (from 30 °C to 110 °C, see legend) for an OFF-state drain-source voltage ($V_{DS,OFF}$) of 25 V. b) Arrhenius plot corresponding to the thermally activated process. The linear fit of the data gives an activation energy E_A≈0.83 eV for both measurements and simulations.

The C doping model employed in this work allowed us to explain measured current-collapse, threshold voltage shifts, and breakdown effects in different GaN power HEMTs [11], [13], [41], [43]–[47]. More details regarding the adopted C doping model, its dependability and its applicability limits are found in [11].

IV. RESULTS AND DISCUSSION

A. Experimental Results

In Fig. 1 the dynamic R_{ON} values measured in the devices under study with the procedure described in Section III.A are compared with data from similar characterizations reported in the literature. Our data specifically refers to room temperature and maximum stress time of 1000 s. The acquired dynamic R_{ON} values were normalized to R_{ON0} in order to allow for the comparison of different devices and technologies. From the data in Fig. 1, we observe that R_{ON} increases up until $V_{DS,OFF}$ reaches the 100-200 V range, and then starts decreasing for higher $V_{DS,OFF}$. This observation suggests that a field-enhanced mechanism comes into play, counteracting the further dynamic R_{ON} increase leading to the reduction of this parameter.

As widely pointed out in the literature, in present GaN power devices the increase in the dynamic R_{ON} compared to the static value can be attributed to the dynamics of buffer traps [7], [17], [19]–[21]. GaN HEMTs considered in this work feature a C-doped buffer, so that the prime suspect is the C_N state. To verify whether the measured dynamic R_{ON} dispersion is actually related to C-doping in the buffer, we performed OFF-state

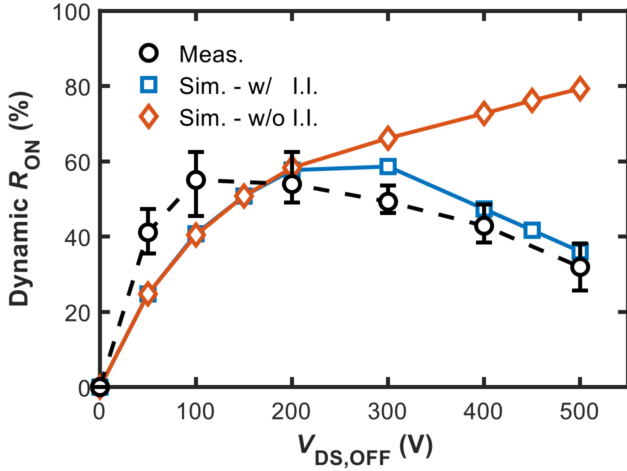

Fig. 6 Comparison between simulated and measured dynamic R_{ON} vs $V_{DS,OFF}$ (see legend). Simulations were carried out with and without Impact Ionization (I.I.). Stress time is t_{OFF}=1000 s for both experiments and simulations.

stress characterization at different temperatures. A thermal chuck (thermally connected to the device via the back metal contact of the package) was used for setting the device temperature during the measurements. A low $V_{DS,OFF}$ value of 25 V was adopted in order to reduce the influence of electric field that could potentially affect the estimation of the activation energy [48]. Typical, measured normalized (R_{ON}/R_{ON0}) transients obtained in the 30 °C to 110 °C temperature range at $V_{DS,OFF}$ = 25 V are reported in Fig. 5(a). Simulated transients for the same temperature range and $V_{DS,OFF}$ are shown in Fig. 5(b). To characterize the activation energy (E_A) of the process, the time constants (τ) of the R_{ON} dynamics were first extracted from the measured and simulated transients at each temperature as follows. First, each transient was fitted with a stretched exponential function [49]; then τ was set in correspondence with the peak of the d(R_{ON}/R_{ON0})/d$\log_{10}t$ signal at each temperature, yielding the Arrhenius plot shown in Fig. 5(c). The linear fit of the measurement/simulation points on the Arrhenius plot yields E_A≈0.83 eV, which is consistent with values reported in the literature for the C_N states [25], [41]. Accordingly, the observed R_{ON} transients can be ascribed to the emission of holes from C_N traps [11], [41]. The corresponding increase of dynamic R_{ON} during transients can thus be interpreted as being due to the negative charge build-up in the buffer layer in the gate-drain access region [9], [11], [14]–[16].

B. Simulation Results

To quantitatively interpret the observed non-monothonic dynamic R_{ON} behavior, see Fig. 1, we performed 2D simulations with the simulation deck described in Sec. III.B. To mimic measurement conditions, stress was held for 1000 s at each $V_{DS,OFF}$ bias and then R_{ON} was evaluated after performing a fast sweep to bias the device in its triode region (V_{GS}=6 V; V_{DS}=0.5 V). Because of the relatively large time constant of R_{ON} transients (due to the slow hole emission process), a total stress time of 1000 s was adopted to properly evaluate the R_{ON} degradation induced by C-related acceptor traps. Simulation results are shown in Fig. 6 along with measurement data points (same already shown in Fig. 1), finding an overall good agreement for the explored $V_{DS,OFF}$ range. The simulations are

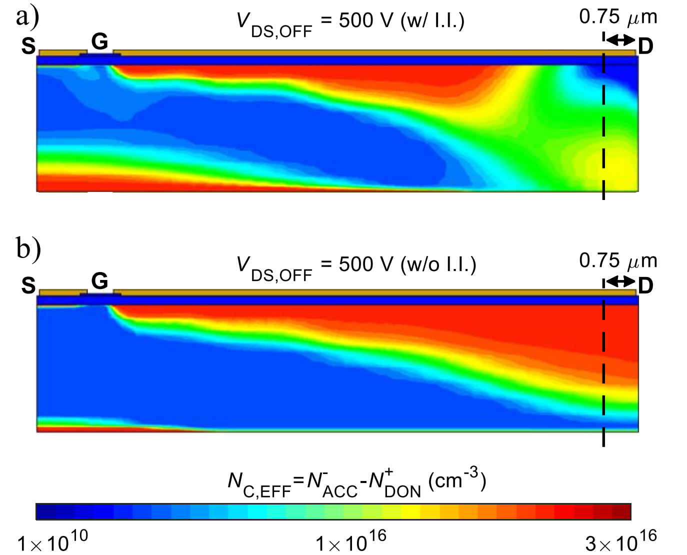

Fig. 7. Simulated *net* ionized acceptor trap density ($N_{C,EFF} = N_{ACC}^- - N_{DON}^+$) in the Carbon-doped GaN buffer (a) with and (b) without Impact Ionization (I.I.) at $V_{DS,OFF}$ = 500 V. The vertical dashed lines indicate the distance from the drain contact (not in scale) of the cutlines used in Fig. 9.

consistent with the observed dynamic R_{ON} decrease that occurs for $V_{DS,OFF}$ ≥ 300 V, see Fig. 6. Interestingly, this behavior can be accounted for by the simulations *only when including* avalanche generation due to impact ionization, as it can be observed by comparing the blue squares with orange diamonds in Fig. 6. This occurs because of the partial neutralization of negatively charged acceptors in the buffer (i.e., N_{ACC}^-) by impact-ionization generated holes that get trapped by these states. The partial reduction of the negatively ionized acceptors increases the 2DEG concentration in the access region, giving rise to the observed R_{ON} reduction. Conversely, when there is no impact ionization activated in the simulations, then the negatively ionized acceptors keep increasing with $V_{DS,OFF}$, hence preventing the partial R_{ON} recovery, see Fig. 6.

Figure 7 shows a contour plot of the net ionized acceptor trap concentration in the buffer, $N_{C,EFF}$, in the case with (a) and without (b) impact ionization activated at $V_{DS,OFF}$ = 500 V. In the first case, see Fig. 7(a), $N_{C,EFF}$ is reduced in the gate-drain access region close to the drain contact compared to the second case, see Fig. 7(b). The region close to the drain conctact where $N_{C,EFF}$ decreases in the first case corresponds to the region where the generated holes are highest, consistently with the explanation for the R_{ON} reduction given above. This can be appreciated in Fig. 8(a) and (b), showing the contour plot of the avalanche generation rate and electric field magnitude, respectively. The peak of generation rate is located near the drain contact, where also the electric field magnitude is highest. Figure 9 shows $N_{C,EFF}$ and the hole current density (Jp) along a vertical cutline in the buffer near the drain contact for the same conditions as in Figs. 7, 8 (i.e., $V_{DS,OFF}$ = 500 V). From Fig. 9 it is evident that only when impact ionization is activated, is there an appreciable amount of generated holes that reduces the ionized acceptor trap density compared to the case when no impact ionization is considered.

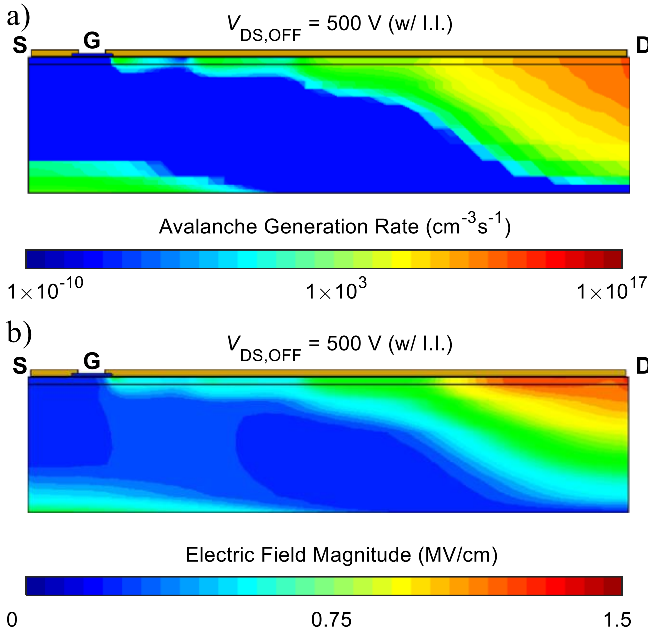

Fig. 8. Simulated (a) avalanche generation rate and (b) electric field magnitude in the device with Impact Ionization (I.I.) at $V_{DS,OFF}$ = 500 V.

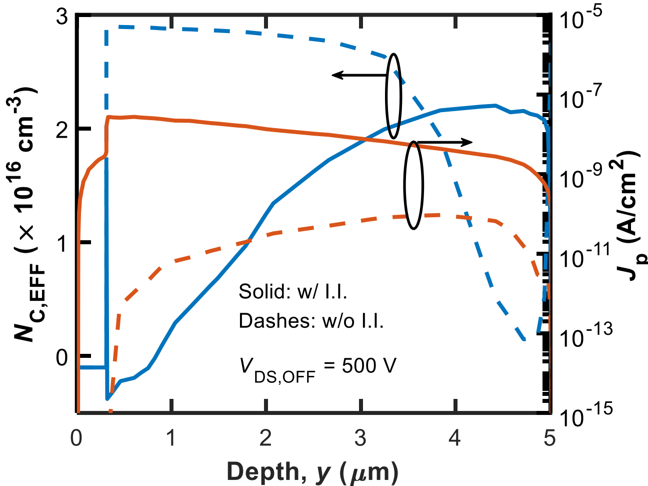

Fig. 9. Simulated $N_{C,EFF}$ (left y-axis) and Jp (right y-axis) along the cut lines indicated in Fig. 7 with and without Impact Ionization (I.I.) at $V_{DS,OFF}$ = 500 V.

C. Discussion

The concept of holes (or more generally, positive charges) compensating the adverse effect of negatively ionized acceptor traps and (partially) suppressing the buffer-induced dynamic R_{ON} degradation at high $V_{DS,OFF}$ was already proposed by other authors [10], [22], [31], [50]. However, the results presented here: *i)* clearly point to hole emission from Carbon acceptor traps as the cause for dynamic R_{ON} degradation [11], [41], see Fig. 5, and *ii*) show by means of calibrated device simulations that holes generated by impact ionization in the high-field region of the buffer and their capture into the same traps are a simple yet physically-sound explanation for the partial suppression of dynamic R_{ON} degradation at large $V_{DS,OFF}$.

Moreover, both experiments and simulations carried out in this work indicate that R_{ON} degradation cannot be associated to electron trapping for two reasons. First, R_{ON} degradation is a thermally activated process as shown in Fig. 5, which cannot be explained by a capture process [11]. Second, and more importantly, as shown in Fig. 4, the fact that leakage current at the drain contact starts increasing for $V_{DS,OFF} \approx 300$ V would lead to more electron trapping and hence to an increase in dynamic R_{ON}, which is opposite to the actual behavior, see Fig. 6.

In general, the degree to which partial dynamic R_{ON} recovery occurs (or does not occur altogether) depends on device technology, structure, Carbon doping auto-compensation (i.e., *net* acceptor trap concentration), switching mode, stress conditions, etc. In this sense, the physical interpretation of impact ionization being the root cause for the non-monotonic dynamic R_{ON} behavior is valid only for devices and/or stress conditions similar to those employed here.

In this work, we limited the dynamic R_{ON} vs $V_{DS,OFF}$ analysis to room temperature only. Although extending the analysis to higher temperatures might clarify the role of impact ionization, the extraction of a clear and unambiguous signature of impact ionization from measurements might not be a trivial task due to the interplay between concurrent mechanisms (such as Poole-Frenkel enhancement of hole emission from acceptor traps [48], [51] and substrate leakage increase [35]) that also are expected to influence the temperature-dependent dynamic R_{ON} vs $V_{DS,OFF}$ behavior. Therefore, temperature analysis of dynamic R_{ON} requires a thorough investigation which will be subject of future work.

Finally, we observe that the reduction of the negative charge in the gate-drain access region due to hole injection through an ad-hoc p-type injector integrated into the device structure as the origin for reduced R_{ON} dispersion was experimentally demonstrated in [52], further validating our interpretation.

V. Conclusions

We provided a quantitative explanation for the non-monotonic dynamic R_{ON} behavior with increasing OFF-state stress bias observed in p-GaN gate AlGaN/GaN power HEMTs. The characterization of the dynamic R_{ON} transients during OFF-state stress allowed the extraction of a 0.83 eV activation energy that correlates very well with the generally assumed, dominant hole trap related to C doping in the device buffer. Based on this result, the increase in the dynamic R_{ON} over its static value has to be attributed to hole detrapping from these buffer traps within the gate-drain access region during the OFF-state phase of the pulse-mode tests. Conversely, the observed R_{ON} recovery at large drain stress bias finds a straightforward interpretation by assuming that holes generated by a high electric field mechanism get trapped in C-related traps thus partially neutralizing the negatively ionized acceptors. This explanation was supported by calibrated 2D numerical simulations that consistently reproduced the dynamic R_{ON} decrease for the explored $V_{DS,OFF}$ range *only when including* hole generation due to impact ionization.

References

[1] J. A. del Alamo and E. S. Lee, "Stability and Reliability of Lateral GaN Power Field-Effect Transistors," *IEEE Trans. Electron Devices*, vol. 66, no. 11, pp. 4578–4590, Nov. 2019. DOI: 10.1109/TED.2019.2931718.

[2] K. J. Chen, O. Haberlen, A. Lidow, C. L. Tsai, T. Ueda, Y. Uemoto, and Y. Wu, "GaN-on-Si power technology: Devices and applications," *IEEE Trans. Electron Devices*, vol. 64, no. 3, pp. 779–795, Mar. 2017. DOI:

10.1109/TED.2017.2657579.

[3] Y. Uemoto, M. Hikita, H. Ueno, H. Matsuo, H. Ishida, M. Yanagihara, T. Ueda, T. Tanaka, and D. Ueda, "Gate injection transistor (GIT) - A normally-off AlGaN/GaN power transistor using conductivity modulation," *IEEE Trans. Electron Devices*, vol. 54, no. 12, pp. 3393–3399, 2007. DOI: 10.1109/TED.2007.908601.

[4] O. Hilt, F. Brunner, E. Cho, A. Knauer, E. Bahat-Treidel, and J. Wurfl, "Normally-off high-voltage p-GaN gate GaN HFET with carbon-doped buffer," in *IEEE International Symposium on Power Semiconductor Devices and ICs (ISPSD)*, May 2011, pp. 239–242. DOI: 10.1109/ISPSD.2011.5890835.

[5] H. Amano, Y. Baines, E. Beam, M. Borga, T. Bouchet, P. R. Chalker, M. Charles, K. J. Chen, N. Chowdhury, R. Chu, C. De Santi, M. M. De Souza, S. Decoutere, L. Di Cioccio, B. Eckardt, T. Egawa, P. Fay, J. J. Freedsman, L. Guido, O. Häberlen, G. Haynes, T. Heckel, D. Hemakumara, P. Houston, J. Hu, M. Hua, Q. Huang, A. Huang, S. Jiang, H. Kawai, D. Kinzer, M. Kuball, A. Kumar, K. B. Lee, X. Li, D. Marcon, M. März, R. McCarthy, G. Meneghesso, M. Meneghini, E. Morvan, A. Nakajima, E. M. S. Narayanan, S. Oliver, T. Palacios, D. Piedra, M. Plissonnier, R. Reddy, M. Sun, I. Thayne, A. Torres, N. Trivellin, V. Unni, M. J. Uren, M. Van Hove, D. J. Wallis, J. Wang, J. Xie, S. Yagi, S. Yang, C. Youtsey, R. Yu, E. Zanoni, S. Zeltner, and Y. Zhang, "The 2018 GaN power electronics roadmap," *J. Phys. D. Appl. Phys.*, vol. 51, no. 16, p. 163001, 2018. DOI: 10.1088/1361-6463/aaaf9d.

[6] L. Sayadi, G. Iannaccone, S. Sicre, O. Haberlen, and G. Curatola, "Threshold Voltage Instability in p-GaN Gate AlGaN/GaN HFETs," *IEEE Trans. Electron Devices*, vol. 65, no. 6, pp. 2454–2460, Jun. 2018. DOI: 10.1109/TED.2018.2828702.

[7] E. Canato, M. Meneghini, C. De Santi, F. Masin, A. Stockman, P. Moens, E. Zanoni, and G. Meneghesso, "OFF-state trapping phenomena in GaN HEMTs: Interplay between gate trapping, acceptor ionization and positive charge redistribution," *Microelectron. Reliab.*, vol. 114, no. May, p. 113841, 2020. DOI: 10.1016/j.microrel.2020.113841.

[8] E. Bahat-Treidel, F. Brunner, O. Hilt, E. Cho, J. Würfl, and G. Trankle, "AlGaN/GaN/GaN:C back-barrier HFETs with breakdown voltage of over 1 kV and low RON× A," *IEEE Trans. Electron Devices*, vol. 57, no. 11, pp. 3050–3058, Nov. 2010. DOI: 10.1109/TED.2010.2069566.

[9] G. Meneghesso, M. Meneghini, I. Rossetto, D. Bisi, S. Stoffels, M. Van Hove, S. Decoutere, and E. Zanoni, "Reliability and parasitic issues in GaN-based power HEMTs: a review," *Semicond. Sci. Technol.*, vol. 31, no. 9, p. 093004, Sep. 2016. DOI: 10.1088/0268-1242/31/9/093004.

[10] M. J. Uren, S. Karboyan, I. Chatterjee, A. Pooth, P. Moens, A. Banerjee, and M. Kuball, "'Leaky Dielectric' Model for the Suppression of Dynamic RON in Carbon-Doped AlGaN/GaN HEMTs," *IEEE Trans. Electron Devices*, vol. 64, no. 7, pp. 2826–2834, Jul. 2017. DOI: 10.1109/TED.2017.2706090.

[11] N. Zagni, A. Chini, F. M. Puglisi, M. Meneghini, G. Meneghesso, E. Zanoni, P. Pavan, and G. Verzellesi, "'Hole Redistribution' Model Explaining the Thermally Activated RON Stress/Recovery Transients in Carbon-Doped AlGaN/GaN Power MIS-HEMTs," *IEEE Trans. Electron Devices*, vol. 68, no. 2, pp. 697–703, Feb. 2021. DOI: 10.1109/TED.2020.3045683.

[12] M. J. Uren, J. Moreke, and M. Kuball, "Buffer design to minimize current collapse in GaN/AlGaN HFETs," *IEEE Trans. Electron Devices*, vol. 59, no. 12, pp. 3327–3333, 2012. DOI: 10.1109/TED.2012.2216535.

[13] N. Zagni, F. M. Puglisi, P. Pavan, A. Chini, and G. Verzellesi, "Insights into the off-state breakdown mechanisms in power GaN HEMTs," *Microelectron. Reliab.*, vol. 100–101, p. 113374, Sep. 2019. DOI: 10.1016/j.microrel.2019.06.066.

[14] D. Bisi, M. Meneghini, F. A. Marino, D. Marcon, S. Stoffels, M. Van Hove, S. Decoutere, G. Meneghesso, and E. Zanoni, "Kinetics of Buffer-Related RON-Increase in GaN-on-Silicon MIS-HEMTs," *IEEE Electron Device Lett.*, vol. 35, no. 10, pp. 1004–1006, Oct. 2014. DOI: 10.1109/LED.2014.2344439.

[15] P. Moens, P. Vanmeerbeek, A. Banerjee, J. Guo, C. Liu, P. Coppens, A. Salih, M. Tack, M. Caesar, M. J. Uren, M. Kuball, M. Meneghini, G. Meneghesso, and E. Zanoni, "On the impact of carbon-doping on the dynamic Ron and off-state leakage current of 650V GaN power devices," *Proc. Int. Symp. Power Semicond. Devices ICs*, vol. 2015-June, pp. 37–40, 2015. DOI: 10.1109/ISPSD.2015.7123383.

[16] K. Tanaka, M. Ishida, T. Ueda, and T. Tanaka, "Effects of Deep Trapping States at High Temperatures on Transient Performance of AlGaN/GaN Heterostructure Field-Effect Transistors," *Jpn. J. Appl. Phys.*, vol. 52, no. 4S, p. 04CF07, Apr. 2013. DOI: 10.7567/JJAP.52.04CF07.

[17] S. Karboyan, M. J. Uren, Manikant, J. W. Pomeroy, and M. Kuball, "On the origin of dynamic Ron in commercial GaN-on-Si HEMTs," *Microelectron. Reliab.*, vol. 81, pp. 306–311, 2018. DOI: 10.1016/j.microrel.2017.10.006.

[18] S. Li, S. Yang, S. Han, and K. Sheng, "Investigation of Temperature-Dependent Dynamic RONof GaN HEMT with Hybrid-Drain under Hard and Soft Switching," *Proc. Int. Symp. Power Semicond. Devices ICs*, vol. 2020-Septe, pp. 306–309, Sep. 2020. DOI: 10.1109/ISPSD46842.2020.9170048.

[19] P. Moens, A. Banerjee, M. J. Uren, M. Meneghini, S. Karboyan, I. Chatterjee, P. Vanmeerbeek, M. Casar, C. Liu, A. Salih, E. Zanoni, G. Meneghesso, M. Kuball, and M. Tack, "Impact of buffer leakage on intrinsic reliability of 650V AlGaN/GaN HEMTs," in *2015 IEEE International Electron Devices Meeting (IEDM)*, Dec. 2015, pp. 35.2.1-35.2.4. DOI: 10.1109/IEDM.2015.7409831.

[20] G. Meneghesso, M. Meneghini, R. Silvestri, P. Vanmeerbeek, P. Moens, and E. Zanoni, "High voltage trapping effects in GaN-based metal-insulator-semiconductor transistors," *Jpn. J. Appl. Phys.*, vol. 55, no. 1, 2016. DOI: 10.7567/JJAP.55.01AD04.

[21] M. J. Uren, M. Caesar, S. Karboyan, P. Moens, P. Vanmeerbeek, and M. Kuball, "Electric Field Reduction in C-Doped AlGaN/GaN on Si High Electron Mobility Transistors," *IEEE Electron Device Lett.*, vol. 36, no. 8, pp. 826–828, 2015. DOI: 10.1109/LED.2015.2442293.

[22] P. Moens, M. J. Uren, A. Banerjee, M. Meneghini, B. Padmanabhan, W. Jeon, S. Karboyan, M. Kuball, G. Meneghesso, E. Zanoni, and M. Tack, "Negative Dynamic Ron in AlGaN/GaN Power Devices," in *IEEE International Symposium on Power Semiconductor Devices and IC's (ISPSD)*, Jun. 2017, pp. 97–100. DOI: 10.23919/ISPSD.2017.7988902.

[23] M. J. Uren and M. Kuball, "Impact of carbon in the buffer on power switching GaN-on-Si and RF GaN-on-SiC HEMTs," *Jpn. J. Appl. Phys.*, vol. 60, no. SB, p. SB0802, 2021. DOI: 10.35848/1347-4065/abdb82.

[24] S. Yang, S. Han, K. Sheng, and K. J. Chen, "Dynamic On-Resistance in GaN Power Devices: Mechanisms, Characterizations, and Modeling," *IEEE J. Emerg. Sel. Top. Power Electron.*, vol. 7, no. 3, pp. 1425–1439, 2019. DOI: 10.1109/JESTPE.2019.2925117.

[25] M. Meneghini, A. Tajalli, P. Moens, A. Banerjee, E. Zanoni, and G. Meneghesso, "Trapping phenomena and degradation mechanisms in GaN-based power HEMTs," *Mater. Sci. Semicond. Process.*, vol. 78, pp. 118–126, May 2018. DOI: 10.1016/j.mssp.2017.10.009.

[26] G. Tang, J. Wei, Z. Zhang, X. Tang, M. Hua, H. Wang, and K. J. Chen, "Dynamic RON of GaN-on-Si Lateral Power Devices With a Floating Substrate Termination," *IEEE Electron Device Lett.*, vol. 38, no. 7, pp. 937–940, Jul. 2017. DOI: 10.1109/LED.2017.2707529.

[27] G. Greco, F. Iucolano, S. Di Franco, C. Bongiorno, A. Patti, and F. Roccaforte, "Effects of Annealing Treatments on the Properties of Al/Ti/p-GaN Interfaces for Normally off p-GaN HEMTs," *IEEE Trans. Electron Devices*, vol. 63, no. 7, pp. 2735–2741, 2016. DOI: 10.1109/TED.2016.2563498.

[28] F. Iucolano, G. Greco, and F. Roccaforte, "Correlation between microstructure and temperature dependent electrical behavior of annealed Ti/Al/Ni/Au Ohmic contacts to AlGaN/GaN heterostructures," *Appl. Phys. Lett.*, vol. 103, no. 20, p. 201604, Nov. 2013. DOI: 10.1063/1.4828839.

[29] M. Moschetti, C. Miccoli, P. Fiorenza, G. Greco, F. Roccaforte, S. Reina, A. Parisi, and F. Iucolano, "Study of behavior of p-gate in Power GaN under positive voltage," in *International Conference of Electrical and Electronic Technologies for Automotive (AEIT)*, 2020. DOI: 10.23919/aeitautomotive50086.2020.9307380.

[30] M. Cioni, A. Bertacchini, A. Mucci, N. Zagni, G. Verzellesi, P. Pavan, and A. Chini, "Evaluation of vth and ron drifts during switch-mode operation in packaged SiC MOSFETs," *Electronics*, vol. 10, no. 4, pp. 1–12, Feb. 2021. DOI: 10.3390/ electronics10040441.

[31] E. Fabris, M. Meneghini, C. De Santi, M. Borga, Y. Kinoshita, K. Tanaka, H. Ishida, T. Ueda, G. Meneghesso, and E. Zanoni, "Hot-Electron Trapping and Hole-Induced Detrapping in GaN-Based GITs and HD-GITs," *IEEE Trans. Electron Devices*, vol. 66, no. 1, pp. 337–342, Jan. 2019. DOI: 10.1109/TED.2018.2877905.

[32] Synopsys, "Sentaurus SDevice Manual (N-2017.09)." 2017.

[33] B. Bakeroot, A. Stockman, N. Posthuma, S. Stoffels, and S. Decoutere, "Analytical model for the threshold voltage of p-(Al)GaN high-electron-mobility transistors," *IEEE Trans. Electron Devices*, vol. 65, no. 1, pp. 79–86, Jan. 2018. DOI: 10.1109/TED.2017.2773269.

[34] V. Joshi, A. Soni, S. P. Tiwari, and M. Shrivastava, "A Comprehensive Computational Modeling Approach for AlGaN/GaN HEMTs," *IEEE Trans. Nanotechnol.*, vol. 15, no. 6, pp. 947–955, Nov. 2016. DOI: 10.1109/TNANO.2016.2615645.

[35] D. Cornigli, S. Reggiani, E. Gnani, A. Gnudi, G. Baccarani, P. Moens, P. Vanmeerbeek, A. Banerjee, and G. Meneghesso, "Numerical Investigation of

the Lateral and Vertical Leakage Currents and Breakdown Regimes in GaN-on-Silicon Vertical Structures," in *IEEE International Electron Devices Meeting (IEDM)*, 2015, pp. 109–112. ISBN: 9781467398947.

[36] M. Borga, C. De Santi, S. Stoffels, B. Bakeroot, X. Li, M. Zhao, M. Van Hove, S. Decoutere, G. Meneghesso, M. Meneghini, and E. Zanoni, "Modeling of the Vertical Leakage Current in AlN/Si Heterojunctions for GaN Power Applications," *IEEE Trans. Electron Devices*, vol. 67, no. 2, pp. 595–599, Feb. 2020. DOI: 10.1109/TED.2020.2964060.

[37] E. Bellotti and F. Bertazzi, "A numerical study of carrier impact ionization in Al xGa 1-xN," *J. Appl. Phys.*, vol. 111, no. 10, p. 103711, May 2012. DOI: 10.1063/1.4719967.

[38] J. L. Lyons, A. Janotti, and C. G. Van De Walle, "Effects of carbon on the electrical and optical properties of InN, GaN, and AlN," *Phys. Rev. B - Condens. Matter Mater. Phys.*, vol. 89, no. 3, pp. 1–8, Jan. 2014. DOI: 10.1103/PhysRevB.89.035204.

[39] M. Matsubara and E. Bellotti, "A first-principles study of carbon-related energy levels in GaN. I. Complexes formed by substitutional/interstitial carbons and gallium/nitrogen vacancies," *J. Appl. Phys.*, vol. 121, no. 19, p. 195701, May 2017. DOI: 10.1063/1.4983452.

[40] A. Armstrong, C. Poblenz, D. S. Green, U. K. Mishra, J. S. Speck, and S. A. Ringel, "Impact of substrate temperature on the incorporation of carbon-related defects and mechanism for semi-insulating behavior in GaN grown by molecular beam epitaxy," *Appl. Phys. Lett.*, vol. 88, no. 8, pp. 1–4, Feb. 2006. DOI: 10.1063/1.2179375.

[41] A. Chini, G. Meneghesso, M. Meneghini, F. Fantini, G. Verzellesi, A. Patti, and F. Iucolano, "Experimental and Numerical Analysis of Hole Emission Process from Carbon-Related Traps in GaN Buffer Layers," *IEEE Trans. Electron Devices*, vol. 63, no. 9, pp. 3473–3478, Sep. 2016. DOI: 10.1109/TED.2016.2593791.

[42] V. Joshi, S. P. Tiwari, and M. Shrivastava, "Part I: Physical Insight Into Carbon-Doping-Induced Delayed Avalanche Action in GaN Buffer in AlGaN/GaN HEMTs," *IEEE Trans. Electron Devices*, vol. 66, no. 1, pp. 561–569, Jan. 2019. DOI: 10.1109/TED.2018.2878770.

[43] G. Verzellesi, L. Morassi, G. Meneghesso, M. Meneghini, E. Zanoni, G. Pozzovivo, S. Lavanga, T. Detzel, O. Häberlen, and G. Curatola, "Influence of buffer carbon doping on pulse and AC behavior of insulated-gate field-plated power AlGaN/GaN HEMTs," *IEEE Electron Device Lett.*, vol. 35, no. 4, pp. 443–445, 2014. DOI: 10.1109/LED.2014.2304680.

[44] G. Meneghesso, R. Silvestri, M. Meneghini, A. Cester, E. Zanoni, G. Verzellesi, G. Pozzovivo, S. Lavanga, T. Detzel, O. Haberlen, and G. Curatola, "Threshold voltage instabilities in D-mode GaN HEMTs for power switching applications," in *IEEE International Reliability Physics Symposium (IRPS)*, 2014, pp. 6–10. DOI: 10.1109/IRPS.2014.6861109.

[45] N. Zagni, A. Chini, F. M. Puglisi, P. Pavan, and G. Verzellesi, "The Role of Carbon Doping on Breakdown, Current Collapse, and Dynamic On-Resistance Recovery in AlGaN/GaN High Electron Mobility Transistors on Semi-Insulating SiC Substrates," *Phys. status solidi*, vol. 217, p. 1900762, Dec. 2019. DOI: 10.1002/pssa.201900762.

[46] N. Zagni, A. Chini, F. M. Puglisi, P. Pavan, M. Meneghini, G. Meneghesso, E. Zanoni, and G. Verzellesi, "Trap Dynamics Model Explaining the R ON Stress/Recovery Behavior in Carbon-Doped Power AlGaN/GaN MOS-HEMTs," in *2020 IEEE International Reliability Physics Symposium (IRPS)*, Apr. 2020, pp. 1–5. DOI: 10.1109/IRPS45951.2020.9128816.

[47] N. Zagni, A. Chini, F. M. Puglisi, P. Pavan, and G. Verzellesi, "The effects of carbon on the bidirectional threshold voltage instabilities induced by negative gate bias stress in GaN MIS-HEMTs," *J. Comput. Electron.*, vol. 19, no. 4, pp. 1555–1563, Dec. 2020. DOI: 10.1007/s10825-020-01573-8.

[48] X. Chen, Y. Zhong, Y. Zhou, H. Gao, X. Zhan, S. Su, X. Guo, Q. Sun, Z. Zhang, W. Bi, and H. Yang, "Determination of carbon-related trap energy level in (Al)GaN buffers for high electron mobility transistors through a room-temperature approach," *Appl. Phys. Lett.*, vol. 117, no. 26, 2020. DOI: 10.1063/5.0031029.

[49] D. Bisi, M. Meneghini, C. De Santi, A. Chini, M. Dammann, P. Bruckner, M. Mikulla, G. Meneghesso, and E. Zanoni, "Deep-level characterization in GaN HEMTs-Part I: Advantages and limitations of drain current transient measurements," *IEEE Trans. Electron Devices*, vol. 60, no. 10, pp. 3166–3175, 2013. DOI: 10.1109/TED.2013.2279021.

[50] S. Yang, C. Zhou, S. Han, J. Wei, K. Sheng, and K. J. Chen, "Impact of Substrate Bias Polarity on Buffer-Related Current Collapse in AlGaN/GaN-on-Si Power Devices," *IEEE Trans. Electron Devices*, vol. 64, no. 12, pp. 5048–5056, 2017. DOI: 10.1109/TED.2017.2764527.

[51] L. Colalongo, M. Valdinoci, G. Baccarani, P. Migliorato, G. Tallarida, and C. Reita, "Numerical analysis of poly-TFTs under off conditions," *Solid. State. Electron.*, vol. 41, no. 4, pp. 627–633, Apr. 1997. DOI: 10.1016/S0038-1101(96)00201-8.

[52] K. Tanaka, T. Morita, H. Umeda, S. Kaneko, M. Kuroda, A. Ikoshi, H. Yamagiwa, H. Okita, M. Hikita, M. Yanagihara, Y. Uemoto, S. Takahashi, H. Ueno, H. Ishida, M. Ishida, and T. Ueda, "Suppression of current collapse by hole injection from drain in a normally-off GaN-based hybrid-drain-embedded gate injection transistor," *Appl. Phys. Lett.*, vol. 107, no. 16, Oct. 2015. DOI: 10.1063/1.4934184.